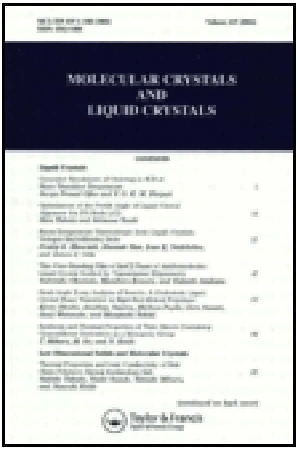

Molecular Crystals and Liquid Crystals
Publication details, including instructions for authors and subscription information:
http://www.tandfonline.com/loi/gmcl20

The Refractive Indices of Nematic Liquid Crystal 4′-n-pentyl-4-cyanobiphenyl in the THz Frequency Range

Ru-Pin Pan [a] , Tsong-Ru Tsai [b] , Chao-Yuan Chen [b] , Chiung-Han Wang [b] & Ci-Ling Pan [b]

[a] Department of Electrophysics , National Chiao Tung University , Hsinchu, Taiwan, R.O.C.

[b] Institute of Electro-Optical Engineering , National Chiao Tung University , Hsinchu, Taiwan, R.O.C.

Published online: 18 Oct 2010.

To cite this article: Ru-Pin Pan , Tsong-Ru Tsai , Chao-Yuan Chen , Chiung-Han Wang & Ci-Ling Pan (2004) The Refractive Indices of Nematic Liquid Crystal 4′-n-pentyl-4-cyanobiphenyl in the THz Frequency Range, Molecular Crystals and Liquid Crystals, 409:1, 137-144, DOI: 10.1080/15421400490431039

To link to this article: http://dx.doi.org/10.1080/15421400490431039

Mol. Cryst. Liq. Cryst., Vol. 409, pp. 137–144, 2004

ISSN: 1542-1406 print/1563-5287 online
DOI: 10.1080/15421400490431039

THE REFRACTIVE INDICES OF NEMATIC LIQUID CRYSTAL 4′-*n*-PENTYL-4-CYANOBIPHENYL IN THE THz FREQUENCY RANGE

Ru-Pin Pan
Department of Electrophysics, National Chiao Tung University, Hsinchu, Taiwan 300, R.O.C.

Tsong-Ru Tsai, Chao-Yuan Chen, Chiung-Han Wang, and Ci-Ling Pan
Institute of Electro-Optical Engineering, National Chiao Tung University, Hsinchu, Taiwan 300, R.O.C.

The terahertz (THz) refractive indices of a liquid crystal 4′-n-pentyl-4-cyanobiphenyl (5CB) in both of the nematic and isotropic phases were determined by terahertz (THz) time-domain spectroscopy for the first time, to our knowledge. We find that the extinction coefficient of 5CB is negligibly small in this frequency range. The birefringence of 5CB, on the other hand, is as large as 0.2. This is comparable to that of 5CB in the visible and near IR. The experimental results indicate that liquid crystals are potentially useful for device applications in the THz frequency range.

Keywords: 5CB; birefringenc; far infrared; Liquid crystal; THz; Time-domain spectroscopy

1. INTRODUCTION

The knowledge of the frequency dependence and the magnitude of the refractive indices as well as the birefringence ($\Delta n = n_e - n_o$) of liquid crystals (LCs) is a key for both fundamental studies and practical applications of LCs. Many groups have investigated the birefringence of LCs in the visible [1–5]. In the infrared, the refractive indices and other optical properties of LCs have also been reported [6–9]. In the millimeter wave range, Lim

This work was supported in part by the National Science Council of R.O.C. under Grants No. NSC 89-2218-E-009-061, 90-2112-M-009-051 and -053. T. R. Tsai and C.-L. Pan were also supported by the Pursuit of Academic Excellence Program of Ministry of Education, R.O.C.
*Corresponding author. E-mail: rpchapo@mail.nctu.edu.tw

et al. [10] first showed that many LCs have comparatively large birefringence with approximate values in the of 0.1–0.18 range at 30 GHz. Further, the birefringence of LCs varied only slightly in the 15–94 GHz range. Based on this, liquid-crystal-based waveguide-type or microstrip-type phase shifters in millimeter wave regions have been demonstrated [10–12]. In the submillimeter wave range, the refractive indices and transmission losses for some nematic LCs, including 4′-n-pentyl-4-cyanobiphenyl (5CB), have been measured by Nose *et al.* [13] at three discrete wavelengths (118, 215, and 435 μm): The refractive indices of 5CB for ordinary (n_o) and extraordinary rays (n_e) in the submillimeter wave region were found to be slightly larger than those in the visible range. A large birefringence comparable to that in the visible range was also reported. In this work, we employ THz time-domain spectroscopy to determine the refractive indices of 5CB. The refractive indices of 5CB in the frequency range of 0.2 to 0.8 THz are reported.

2. EXPERIMENTAL AND CALCULATION METHODS

The LC sample cell was prepared by sandwiching the commercial available 5CB (Merck) between two fused silica windows. The thickness of the LC layer was controlled by mylar spacers and measured to be 119 μm by using an interference method [14,15]. Homogeneous alignment of the nematic LC was achieved by rubbing the spin coated polyimide films on the substrates. The cell was mounted in a copper oven. The temperature was stabilized within ± 0.1°C.

The time-domain spectroscopy experimental setup shown in Figure 1 is similar to the conventional one and has been described in detail elsewhere [16]. Briefly, a mode-locked Ti: Sapphire laser ($\lambda = 800$ nm) generating $\sim$35 fs pulses at a repetition rate of 80 MHz with 400 mW average output power is used as the light source. The laser beam is divided into two beams, a pump and a probe. A large-aperture photoconductive antenna is used as a THz emitter in our THz spectrometer. The antenna was made from an arsenic-ion-implanted- GaAs wafer with two AuGe electrodes separated by about 2 mm. It was biased at about 800 V. The pump beam illuminates the area between the two electrodes with focused ultrashort laser pulses to produce synchronous bursts of THz wave. The THz wave is collimated and focused on the sample by a pair of off-axis paraboloidal mirrors. The transmitted THz wave through the sample is collimated by a second pair of off-axis paraboloidal mirrors and probed by the delayed probe beam and the electro-optic sampling set up. A 2-mm-thick (110) ZnTe crystal is used for sensing the THz wave.

In this study, a 5CB layer of thickness L, referred as medium 2, is sandwiched between two fused silica substrates (referred to as media 1 and 3).

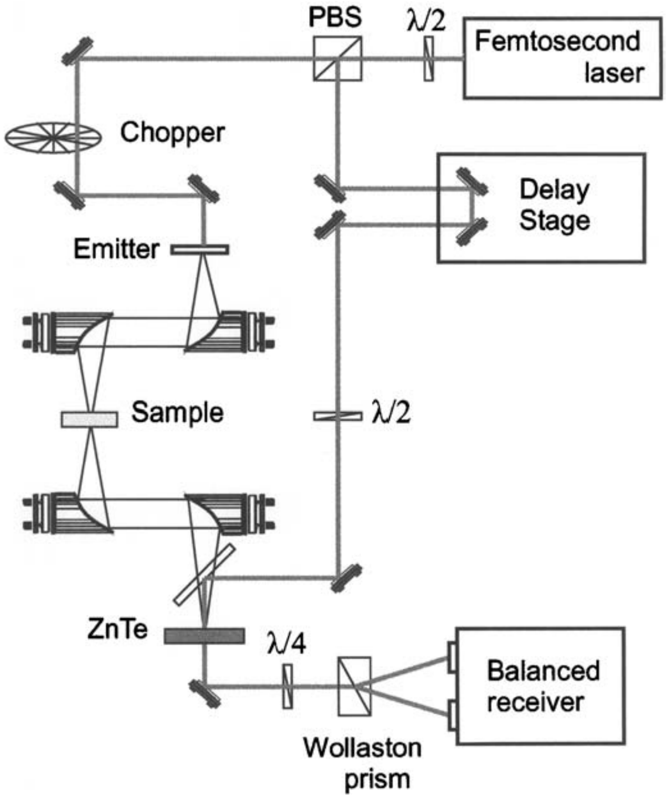

FIGURE 1 The schematic experimental setup for THz transmission measurements. PBS: polarizing beam splitter; $\lambda/2$: half-wave plate; $\lambda/4$: quarter wave plate.

The THz wave transmits through the cell from medium 1 to medium 3. Assuming that the THz wave is a plane wave, the electric field of the THz wave transmitted through the LC cell can be written as:

$$E_{sample}(\omega) = T_{12}(\omega)P_2(\omega, L)T_{23}(\omega) \cdot \sum_{k=0}^{\infty} \{R_{23}(\omega)P_2^2(\omega, L)R_{21}(\omega)\}^k \cdot E(\omega), \tag{1}$$

where $E(\omega)$ is the incident electric field of the THz wave, R_{ij} is the reflection coefficient at the i-j interface, T_{ij} is the transmission coefficient from medium i to medium j and P_2 is the propagation coefficient in medium 2 over a distance L. The definitions for these coefficients are

$$R_{ij} = (n_i - n_j)/(n_i + n_j),$$

$$T_{ij} = 2n_i/(n_i + n_j),$$

and $P_2 = i^{n_2 \omega L}/c$,
with the complex refractive index of medium $2, n_2(\omega)$. The spectral component of the electric field of the THz wave transmitted without the sample is given by

$$E_{ref}(\omega) = T_{1,air}(\omega)T_{air,3}(\omega)\exp(iP_{air})E(\omega)/ [1 + R_{air,1}(\omega)R_{air,3}(\omega)\exp(2iP_{air})]. \quad (2)$$

The complex transmission coefficient $T(\omega)$ of the sample is obtained by dividing the signal E_{sample} recorded with the sample by E_{ref} recorded without the sample,

$$T(\omega) = E_{sample}(\omega)/E_{ref}(\omega). \quad (3)$$

In our case, n_1 and n_3 are index of refraction of the fused silica substrate, which was measured separately. The optical constants of LC can be obtained by solving Eq. (3) with measured $T(\omega)$, numerically [17].

Since a nematic LC can be viewed as a uniaxial crystal [18], two principal refractive indices, $n_e(\omega)$and $n_o(\omega)$, of nematic LC can be defined by the direction of the linearly polarized THz beam being parallel to the LC director or perpendicular to it. The measurements proceeded as follows. First, a reference of the temporal THz waveform was obtained by introducing a vacant cell between the THz emitter and the receiver. Subsequently, the vacant cell was replaced by the LC filled cell and a second set of waveforms was taken. The information for n_e and n_o can be obtained by rotating the cell to adjust the director being parallel to or perpendicular to the polarization direction of THz wave, respectively.

RESULTS AND DISCUSSIONS

A typical set of the temporal THz waveforms transmitted through the samples is shown in Figure 2. The three curves are those from a vacant cell, and a LC cell for which the director of the nematic 5CB is parallel and perpendicular to the direction of polarization of incident THz wave, respectively. Relative small but discernable phase shift can be seen for the latter two cases. The refractive indices of 5CB are then calculated.

Three sets of data for the real part of the refractive index of 5CB in the nematic and isotropic phases are shown in Figure 3. The THz transmission measurements for 5CB in the nematic and isotropic phases were done at 25°C and 38°C, respectively. No sharp resonances, corresponding to absorption peaks, were observed in the frequency range from 0.3 to 0.8 THz.

The real part of the refractive indices of 5CB in the nematic and isotropic phases, n_e, n_o and n_{iso}, all exhibit an increasing trend with frequency. The values of n_{iso} fall between n_e and n_o, in good agreement with the relation, $n_{iso} = (n_e + 2n_o)/3$. For comparison, we also display the discrete values of n_e and n_o at 118, 215, and 435 μm, reported in Reference [13]. Both n_e and n_o reported in this work are somewhat smaller than theirs. The thickness of the LC cell must be measured as accurately as possible, since this quantity enters directly into the determination of the refractive index. In our case, the thickness of the LC layer was measured by an interferometric method [14–15]. The thickness of fused silica window was measured using a universal measuring machine (Société d'Instruments de Physiqué, model SIP-1002M), with an accuracy better than 0.1 μm. Maximum uncertainties are $\delta n \approx \pm 0.01$ and $\delta \kappa \approx \pm 0.005$.

We have also determined the extinction coefficients (the imaginary part of complex refractive indices) of 5CB. These are very small in this frequency range and are shown in Figure 4. The frequency dependence of birefringence Δn of 5CB is shown in Figure 5. It increases with frequency from 0.14 to 0.19. For comparison, the room-temperature (T = 25°C) birefringence of 5CB measured in the visible ($\lambda = 633$ nm) is 0.18. The

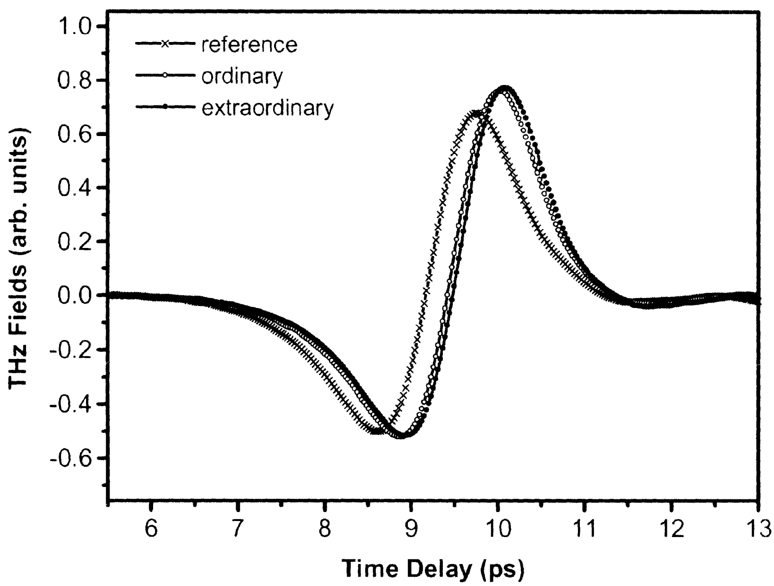

FIGURE 2 Temporal THz waveforms transmitted through a vacant cell, and a LC cell for which the director of the nematic 5CB parallel and perpendicular to the direction of polarization of incident THz wave, respectively.

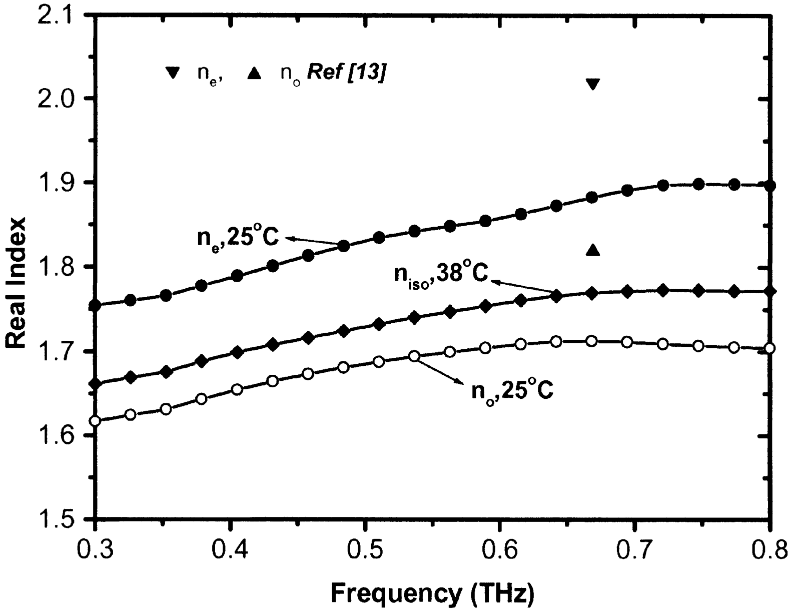

FIGURE 3 The frequency dependence of the real part refractive index of 5CB.

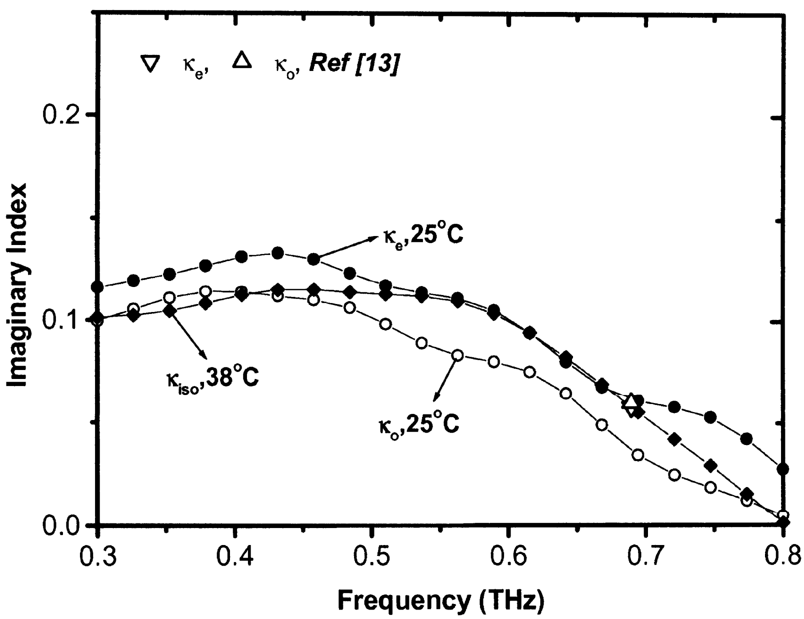

FIGURE 4 The frequency dependence of the imaginary part refractive index of 5CB.

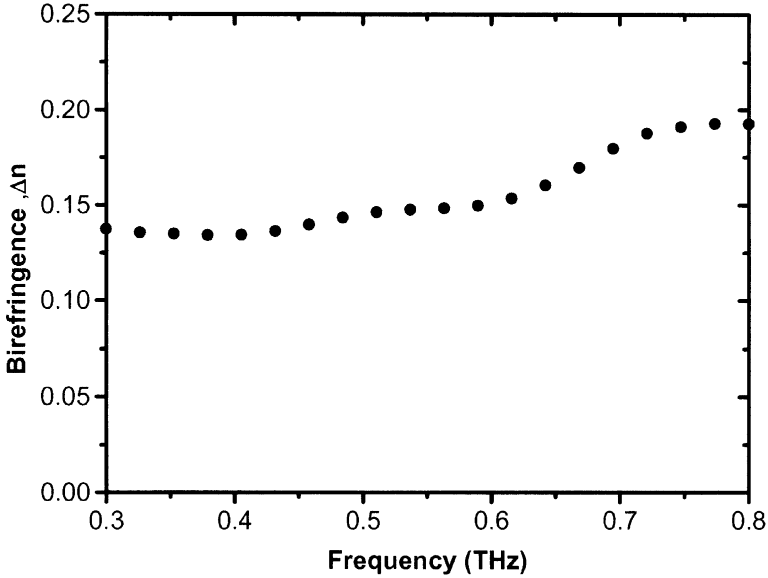

FIGURE 5 The frequency dependence of the birefringence of 5CB.

large birefringence is significant for potential application of LC in THz devices such as phase shifters.

CONCLUSIONS

In conclusion, we have determined the refractive indices of the nematic LC 5CB in the 0.3 to 0.8 THz range by THz time-domain spectroscopy. We find that the extinction of 5CB is negligibly small in this frequency range. The birefringence of 5CB, on the other hand, is as large as 0.19. This is comparable to that of 5CB in the visible and near IR. The experimental results indicate that liquid crystals are potentially useful for device applications in the THz frequency range.

REFERENCES

[1] Chang, R. (1972). *Mater. Res. Bull*, *7*, 267.
[2] Chang, R. (1975). *Mol. Cryst. Liq. Cryst.*, *30*, 155.
[3] Soref, R. A., & Rafuse, M. J. (1972). *J. Appl. Phys.*, *43*, 2029.
[4] Haase, W., & Potzsch, D. (1977). *Mol. Cryst. Liq. Cryst.*, *38*, 77.
[5] Hanson, E. G., & Shen, Y. R. (1976). *Mol. Cryst. Liq. Cryst.*, *36*, 193.
[6] Miraldi, E., Oldano, C., Trossi, L., & Valabrega, P. T. (1982). *Appl. Opt.*, *21*, 4163.

[7] Wu, S. T., Efron, U., & Hess, L. V. (1984). *Appl. Phys. Lett.*, *44*, 1033.
[8] Khoo, I. C., Michael, R. P., & Finn, G. M. (1988). *Appl. Phys. Lett.*, *52*, 2108.
[9] Joffre, P., Illiaquer, G., & Huignard, J. P. (1989). *Proc. SPIE 1126*, 13.
[10] Wu, S. T., Margerum, J. D., Meng, H. B., Hsu, C. S., & Dalton, L. R. (1994). *Appl. Phys. Lett.*, *64*, 1204.
[11] Lim, K. C., Margerum, J. D., Lackner, A. M., Miller, L. J., Sherman, E., & Smith, W. H. (1993). *Liq. Cryst.*, *14*, 327.
[12] Lim, K. C., Margerum, J. D., & Lackner, A. M. (1993). *Appl. Phys. Lett.*. *62*, 1065.
[13] Guérin, F., Chappe, J. M., Joffre, P., & Dolfi, D. (1997). *Jpn. J. Appl. Phys.*, *36*, 4409.
[14] Nose, T., Sato, S., Mizuno, K., Bae J., & Nozokido, T. (1997). *Appl. Opt.*, *36*, 6383.
[15] Yang, K. H. (1988). *J. Appl. Phys.*, *64*, 4780.
[16] Zhu, H., Lin, Q., & Zhang, B. (2000). *Displays*, *21*, 121.
[17] Jiang, Z., Li, M., & Zhang, X.-C. (2000). *Appl. Phys. Lett.*, *76*, 3221.
[18] Duvillaret, L., Garet, F., & Coutaz, J. (1996). *IEEE J. Sel. Top. Quantum Electron.*, *2*, 739.
[19] de Gennes P. G., & Prost, J. (1993). *The Physics of Liquid Crystals*, Oxford University: New York.